THE ROYAL SOCIETY
PUBLISHING

The influence of environmental setting on the community ecology of Ediacaran organisms

Emily G. Mitchell[1], Nikolai Bobkov[2,3], Natalia Bykova[2,4], Alavya Dhungana[5], Anton V. Kolesnikov[2,6,7], Ian R. P. Hogarth[8,†], Alexander G. Liu[9], Tom M. R. Mustill[9,‡], Nikita Sozonov[2,3], Vladimir I. Rogov[2], Shuhai Xiao[4] and Dmitriy V. Grazhdankin[2,3]

[1]Department of Zoology, University of Cambridge, Downing Street, Cambridge CB2 3EJ, UK
[2]Trofimuk Institute of Petroleum Geology and Geophysics, 3, Ac. Koptyuga ave., Novosibirsk 630090, Russian Federation
[3]Novosibirsk State University, Novosibirsk, Novosibirsk Oblast 630090, Russian Federation
[4]Department of Geosciences, Virginia Tech, Blacksburg, VA 24061, USA
[5]Department of Earth Sciences, Durham University, Lower Mountjoy, South Road, Durham DH1 3LE, UK
[6]Geological Institute, Russian Academy of Sciences, Pygevsky 7, Moscow 119017, Russia
[7]Faculty of Geography, Moscow State Pedagogical University, Kibalchicha str. 16, Moscow 129626, Russia
[8]Department of Chemical Engineering, University of Cambridge, Philippa Fawcett Drive, Cambridge CB3 0AS, UK
[9]Department of Earth Sciences, University of Cambridge, Downing Street, Cambridge CB2 3EQ, UK

EGM, 0000-0001-6517-2231; NB, 0000-0003-1876-6445; NB, 0000-0003-4875-5261; AVK, 0000-0003-1028-9082; AGL, 0000-0002-3985-982X; VIR, 0000-0003-1880-5635; SX, 0000-0003-4655-2663; DVG, 0000-0003-0797-1347

The broad-scale environment plays a substantial role in shaping modern marine ecosystems, but the degree to which palaeocommunities were influenced by their environment is unclear. To investigate how broad-scale environment influenced the community ecology of early animal ecosystems, we employed spatial point process analyses (SPPA) to examine the community structure of seven late Ediacaran (558–550 Ma) bedding-plane assemblages drawn from a range of environmental settings and global localities. The studied palaeocommunities exhibit marked differences in the response of their component taxa to sub-metre-scale habitat heterogeneities on the seafloor. Shallow-marine (nearshore) palaeocommunities were heavily influenced by local habitat heterogeneities, in contrast to their deeper-water counterparts. The local patchiness within shallow-water communities may have been further accentuated by the presence of grazers and detritivores, whose behaviours potentially initiated a propagation of increasing habitat heterogeneity of benthic communities from shallow to deep-marine depositional environments. Higher species richness in shallow-water Ediacaran assemblages compared to deep-water counterparts across the studied time-interval could have been driven by this environmental patchiness, because habitat heterogeneities increase species richness in modern marine environments. Our results provide quantitative support for the 'Savannah' hypothesis for early animal diversification—whereby Ediacaran diversification was driven by patchiness in the local benthic environment.

1. Background

The Ediacaran–Cambrian transition (approx. 580–520 million years ago) is one of the most remarkable intervals in the history of life on Earth, witnessing the rise of macroscopic, complex animals in the global oceans [1,2]. The diversification of early animals coincides with dramatic perturbations in the global environment, including changes to carbon cycling and a progressive but dynamic oxygenation of the oceans [3,4]. The extent to which animals themselves drove these global changes is a matter of considerable debate [5–7]. Competing hypotheses

suggested to explain the observed environmental shifts range from global abiotic changes that occurred over kilometre scales [8,9] to biotic factors acting over local scales (metre to kilometre), and include organism interactions such as burrowing and/or predation [10,11]. Feedbacks between biotic and abiotic factors have also been proposed as drivers of early animal diversification, whereby Ediacaran organisms directly or indirectly created patchy food resources, stimulating the evolution of mobile bilaterians [12,13]. Owing to the small (within community) spatial scales over which key evolutionary mechanisms often act [14], investigation of the community ecology of Ediacaran assemblages from sites large distances (kilometres) apart offers an opportunity to link the interactions of individual organisms to macro-evolutionary and macro-ecological trends. In this study, we investigate the relationship between late Ediacaran early animal diversification and the broad-scale environment.

Ediacaran macrofossils occur globally across a wide-range of palaeo-environments [1]. Previous studies have separated late Ediacaran palaeocommunities into three taxonomically distinct assemblages—the Avalon, White Sea and Nama—which occupy partially overlapping temporal intervals and water-depths, with no significant litho-taphonomic or biogeographic influence [15–17]. This study focuses on palaeocommunities within the Avalon and White Sea fossil assemblages. Since these are considered to reflect original in situ communities [18,19], they permit statistical analysis of the distribution of fossil specimens on bedding planes (spatial point process analyses, SPPA), enabling reconstruction of organism interactions with each other and their local environment [20–25]. The Avalon assemblage is primarily represented by sites in Newfoundland (Canada) and Charnwood Forest (UK) [26,27], and typically documents mid-shelf/deep-water settings of approximately 571–557 Ma [28,29]. Such sites exhibit relatively limited ecological and morphological diversity [30,31], and palaeocommunities consist almost exclusively of sessile taxa [32] that show only weak trends in community composition along regional palaeoenvironment gradients [20]. Previous spatial analyses of Avalonian palaeocommunities have found limited evidence for environmental interactions within these communities [21,23], in contrast to the strong imprint exerted by resource-limitation on modern deep-sea ecosystems [33,34].

Palaeocommunities from the White Sea assemblage are most famously represented by sites in South Australia and the East European Platform of Russia, dated to approximately 558–550 Ma [35–37]. These assemblages typically document shallow-water, diverse communities including some of the oldest candidate bilaterians, with taxa interpreted to exhibit a wide range of ecological strategies [7,12,36,38]. Within the White Sea assemblages, community composition is strongly correlated with facies and the presence of textured organic surfaces at bed-scale level [39,40].

Metrics of taxonomic and ecological diversity are much higher in White Sea assemblages than in Avalonian ones, with changes in taxonomic and morphological diversity calculated to be of similar magnitude to those between the Ediacaran and Cambrian [30,31]. These Ediacaran assemblages have high beta-diversity compared to modern benthic systems [41], but the driving processes underlying this high diversity are not understood. The regional palaeoenvironment (kilometre scale) [15,17] has a significant influence on (non-algal dominated) Ediacaran fossil assemblage composition, but its

influence on local (metre to sub-metre scale) community ecology has not yet been investigated. In modern benthic communities, small spatial scale (less than 50 cm) substrate heterogeneities (e.g. substrate variations in nutrients, oxygen patchiness, or biotic and abiotic gradients within microbial mats) exert a significant influence on community ecology [33,34,42]. For Ediacaran palaeocommunities, it is not possible from spatial analyses alone to determine the underlying causes of habitat heterogeneities, nor the extent to which they relate to food resources, such as those resulting from the decay of Ediacaran organisms [12,43]. However, it is possible to compare how the relative influence of such heterogeneities changes with broad-scale environmental setting: previous analyses have identified assemblage-level trends between community compositions and bathymetric depth [15–17]. In this study, we compare the drivers of community ecology between shallow and deep-water Ediacaran palaeocommunities (in nearshore versus offshore depositional environments) over an approximately 8 million year period via spatial analyses of seven palaeocommunities.

1.1. Spatial analyses

Determining the nature of interactions between fossilized organisms and their environment can be undertaken if entire palaeocommunities are preserved in situ, such that the position of a fossil on a bedding plane can be interpreted to reflect aspects of the original organism's life-history [44]. For sessile organisms, such as in the Avalon communities, community-scale spatial distributions are dependent upon the interplay of a limited number of factors: physical environment (which manifests as habitat associations of a taxon or taxon-pairs [45]); organism dispersal/reproduction [46]; competition for resources [47]; facilitation between taxa (where one taxon increases the survival another taxon) [48]; and differential mortality [49]. For fossil assemblages containing mobile taxa (e.g. the White Sea assemblages), behavioural ecology also influences spatial distributions, so interpretations of their spatial distributions are necessarily qualitative rather than quantitative.

Studies of modern ecosystems have demonstrated that habitat associations resulting from interactions between organisms and their local environment can be either positive, leading to aggregations of individuals (such as around a preferential substrate for establishment), or negative segregation away from such patches [21]. SPPA are a suite of analyses which compare the relative density of points (in this case fossil specimens) to different models corresponding to different ecological processes, in order to infer the most likely underlying process responsible for producing the observed spatial distribution [44,50]. The application of SPPA to Ediacaran palaeocommunities is documented in detail in the Methods section (see also [21–23,25,50]). For sessile organisms, habitat associations identified by SPPA are best-modelled by a heterogeneous Poisson model (HP), or when combined with dispersal limitations, an inhomogeneous Thomas cluster model (ITC). Where the local environment is resource limited to the extent that it significantly reduces organism densities, this is indicated by spatial segregation between specimens within a community. When sessile populations are not significantly affected by their local environment, their spatial distributions are completely spatially random (CSR), indicating no significant influence by any biological or ecological processes at the spatial scale investigated [45,51–54]. Alternatively, sessile populations

Table 1. Summary data for the surfaces mapped. The environmental setting, species richness, number of specimens within the mapped area, and the total mapped area are provided.

surface	environmental setting	species richness	dominant taxon/taxa	specimen numbers	area mapped (m^2)
WS-A	shallow	1	*Aspidella*	40	0.54
KH1	deep	2	*Aspidella*	204	2.38
KH2	deep	2	*Aspidella*	81	1.52
DS	shallow	1	*Dickinsonia*	62	9.00
KS	shallow	13	*Kimberella*, *Orbisiana*	80	2.74
FUN4	shallow	2	*Funisia*	290	0.69
FUN5	shallow	1	*Funisia*	482	0.78

which are not CSR and not affected by their local environment reflect dispersal/reproductive processes [45,51–54]. CSR is modelled by homogeneous Poisson processes [44], whereas dispersal patterns are best modelled by best-fit Thomas cluster (TC) or double Thomas cluster (DTC) models [51]. Facilitation (where one taxon increases the survival of another) is best-modelled by linked-cluster models and density-dependent processes are detected using random-labelling analyses [55].

1.2. Geological setting

We assessed the community palaeoecology of seven fossil-bearing assemblages across five different global Ediacaran locations (table 1, figure 1; electronic supplementary material, figure S1), spanning a range of habitats (electronic supplementary material, figure S2) inhabited by members of the Ediacaran soft-bodied macrobiota during the late Edia-caran interval. Data from these assemblages were compared with seven palaeocommunities that have been subjected to SPPA in previous studies (see [21,23] for details of data collection and locality information). The diverse local depositional environments represented by these combined localities are here coarsely grouped within either shallow or deep-water settings, with deep-water defined as those surfaces below storm-wave base (i.e. offshore environments), to permit us to focus attention on the broadest macro-ecological and macro-evolutionary patterns in the data.

1.2.1. Shallow marine settings

Five of the studied palaeocommunities are found in nearshore facies that reflect shallow marine wave and current-agitated depositional environments. Palaeocommunity WS-A (White Sea) is an *Aspidella*–bearing surface (figure 1*e*) on the underside of a 15–30 mm thick wave-rippled sandstone which forms part of a thick package of alternating wave-bedded sandstones, siltstones and mudstones interpreted as a product of progressive sediment-sorting by waves within a prograding, storm-influenced shoreface depositional system (electronic supplementary material, figure S2; [54,56]). It was collected from the Lyamtsa Formation of the Valdai Group, along the Onega Coast of the White Sea, Russian Federation. The original complete surface was studied in the field, where it has since been destroyed by landslides. *Aspidella* specimens were collected and are stored uncatalogued at the Trofimuk Institute of Petroleum Geology and Geophysics in Novosibirsk. The Lyamtsa Formation is older than a date of 558 ± 1 Ma (U/Pb

zircon dating of volcanic tuffs near the base of the overlying Verkhovka Formation) [16].

Surface (KS) (figure 1*a*) originates from a section comprising 1.3–3.2 m thick, laterally continuous fining-upward sequences. Each sequence begins with channel casts or thick (0.5–0.6 m) packages of laterally discontinuous fossiliferous thin-bedded sandstones often exhibiting soft-sediment deformations (electronic supplementary material, figure S2). These are followed by a package (0.4–0.7 m) of interbedded thinner wave-rippled sandstones, progressively thinning towards the top of the package. The upper part of each sequence is represented by an interval of alternating siltstone and shale. This section is interpreted as a prograding flood-influenced prodelta depositional system, and is part of the lower member of the Erga Formation (Winter Coast of the White Sea) [16,35], which is younger than 552.85 ± 0.77 Ma [57] (date recalculated from Martin *et al*. [58]). The KS surface was documented in the field and has subsequently been destroyed by landslides and weathering.

Two *Funisia*-bearing surfaces (figure 1*d*) from oscillation-rippled quartz-sandstones (the 'ORS' facies of [59]) are interpreted to have been deposited between fair-weather and storm-wave base under oscillatory and combined flow in the Ediacara Member of South Australia [39,60–62]. These surfaces reside in the collections of the South Australia Museum, with surface FUN4 collected from Ediacara Conservation Park (SAM P55236) and surface FUN5 collected from the Mount Scott Range (SAM P41506). Since FUN4 and FUN5 originate from different localities (greater than 50 km apart), it is assumed to be likely that they represent discrete bedding plane palaeocommunities. The South Australian Ediacaran successions have not been radiometrically dated, but the Edia-cara Member is widely assumed to be of a similar age to the Russian White Sea fossil-bearing sections [1,2].

Surface DS is a *Dickinsonia*-bearing surface (figure 1*b*) from the Konovalovka Member of the Cherny Kamen Formation, cropping out along the Sylvitsa River, Central Urals, Russian Federation [63,64]. It lies within an interval of finely alternating wave-rippled sandstones, siltstones and mudstones that are sandwiched between two thick intervals of biolaminated sandstone characterized by microbial shrinkage cracks and salt crystal pseudomorphs [65]. The overall succession is considered transitional from marginal marine to non-marine, with the fossil-bearing interval interpreted as having been deposited in a lagoon within a tidal flat depositional system [65]. A U/Pb zircon date of 557 ± 13 Ma from volcanic tuffs near the base of the Cherny Kamen Formation [64] suggests that this unit may
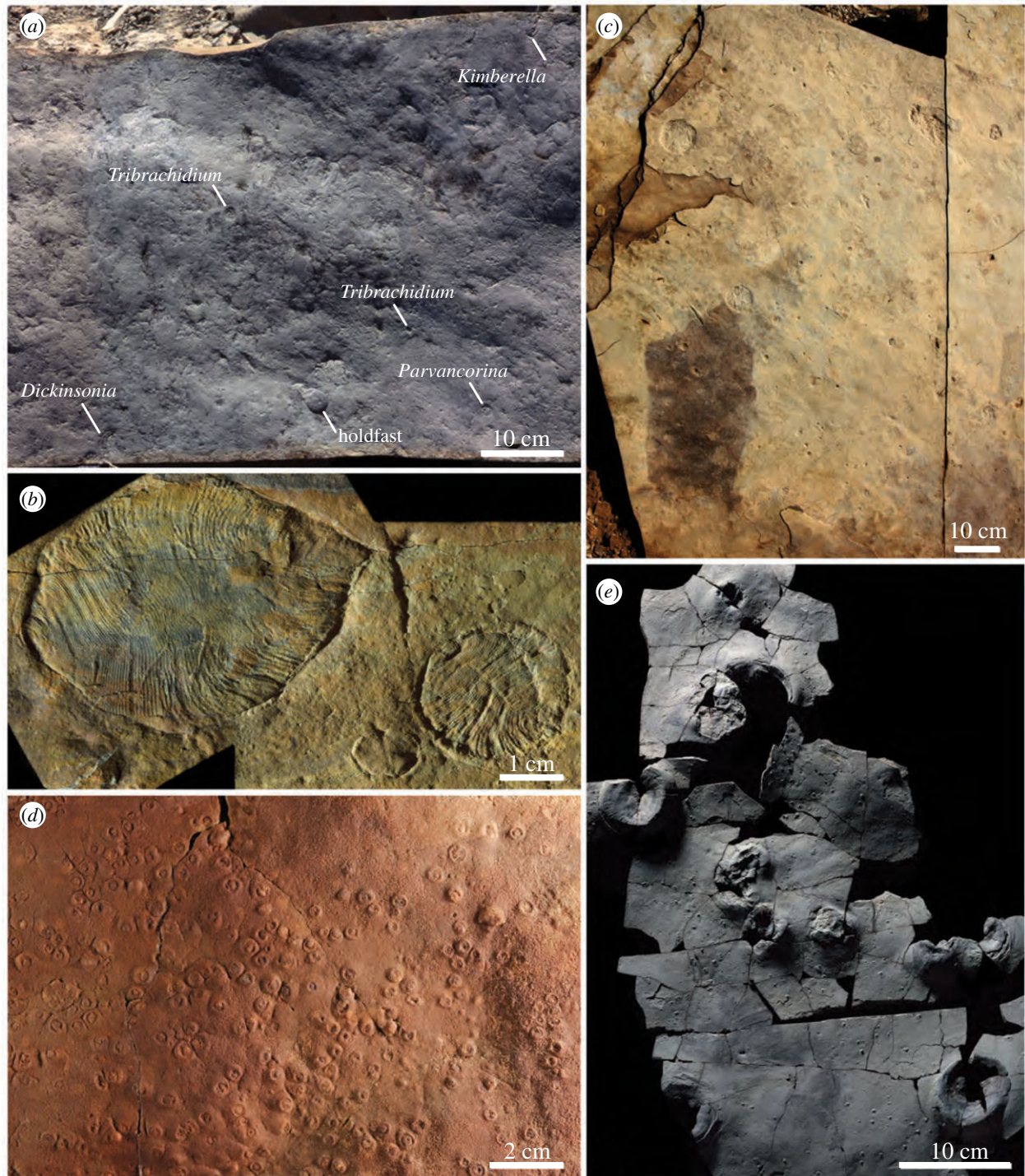
Figure 1. Assemblages of Ediacaran fossils from the study localities. (*a*) A fragment of the Kimberella surface (KS), indicating key taxa, lower Erga Formation, Winter Coast of the White Sea. (*b*) Specimens of *Dickinsonia* from the Dickinsonia surface (DS), Konovalovka Member, Cherny Kamen Formation, Sylvitsa River, Central Urals. (*c*) A representative fragment of the *Aspidella* surface (KH1), Khatyspyt Formation, Olenek Uplift, Northern Siberia. (*d*) *Funisia* from FUN4 surface (SAM P55236), Ediacara Member, Rawnsley Quartzite, South Ediacara Conservation Park, Flinders Ranges, South Australia. (*e*) A representative fragment of the WS-A surface, upper Lyamtsa Formation, White Sea Region. This particular fragment was not included in the analysis.

have been deposited broadly coevally with those on the White Sea coast. Specimens from this surface reside in Trofimuk Institute of Petroleum Geology and Geophysics in Novosibirsk (specimen numbers: 2057-001 to 2057-003) and will be placed at the Ural Geological Museum (Yekaterinburg).

All five of these surfaces, therefore, represent nearshore siliciclastic depositional environments from above the storm-wave base (electronic supplementary material, figure S2), and so fall broadly into the grouping of 'shallow marine'. They contain examples of taxa interpreted as animals (e.g. *Dickinsonia*

[66], *Kimberella* [67]) as well as non-metazoans (*Orbisiana*) [68], and their age and facies place them within the White Sea assemblage [15,17].

1.2.2. Deep marine settings

Two bedding surfaces dominated by *Aspidella* specimens (KH1 and KH2, figure 1*c*) were collected from a package of finely alternating limestone and shale interbeds within the uppermost Khatyspyt Formation, Khorbusuonka River, Siberia. The
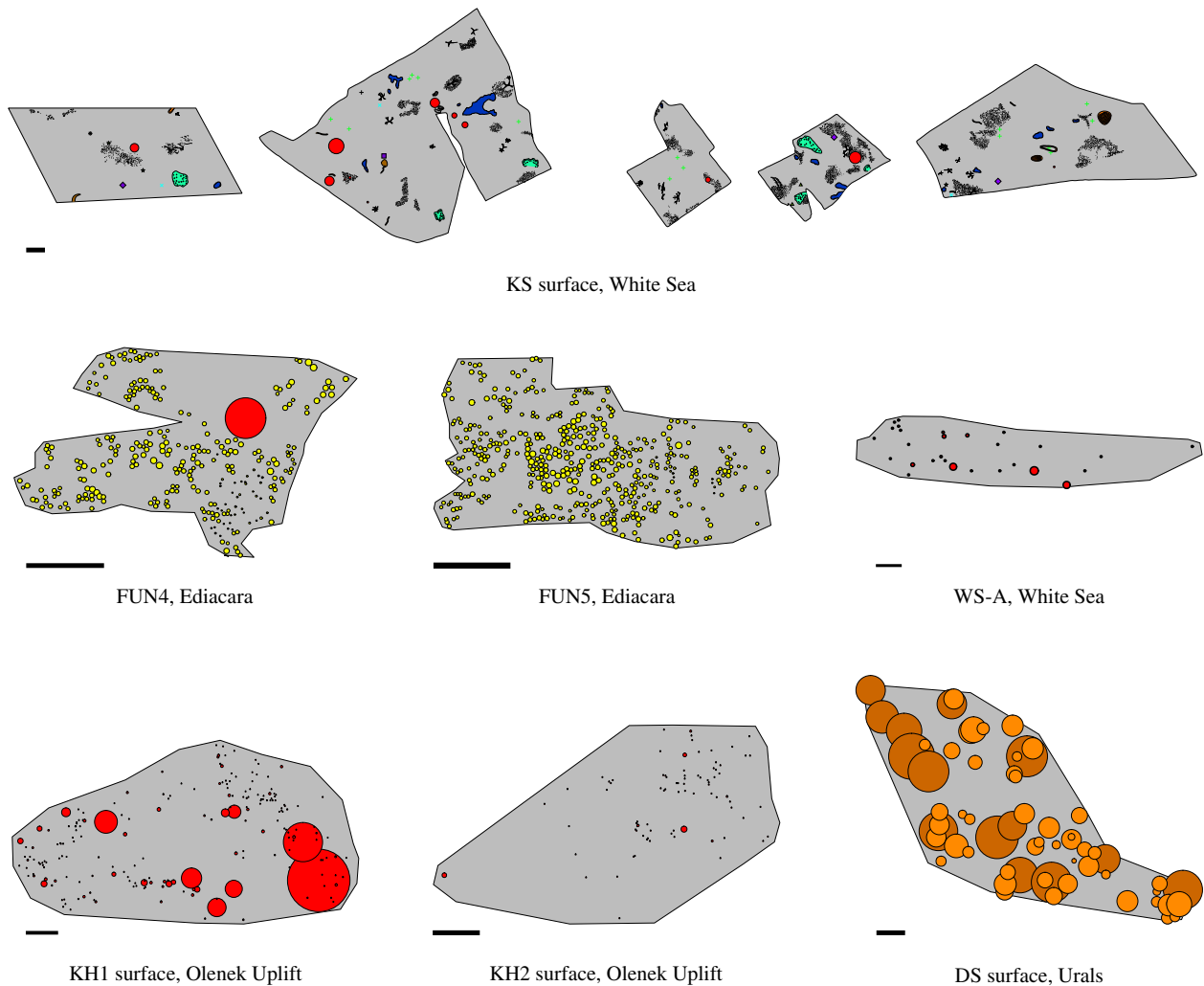
Figure 2. Spatial maps of the seven studied palaeocommunities. Scale bar = 10 cm. Different colours indicate different trace and body fossils as follows: red, *Aspidella*; Orange, *Dickinsonia*; yellow circles, *Funisia*; light green scratch marks, *Kimberichnus*; light green crosses, *Kimberella*; blue crosses, *Charniodiscus*; green triangles, *Parvancorina*; dark blue patches, *Orbisiana*; black stipples, horizontal traces; white globular strings, *Palaeopascichnus*; purple diamonds, *Andiva*; purple squares, *Yorgia*. Size of the circles corresponds to specimen length or diameter (as appropriate). On the DS surface, dark orange circles are the large size class of *Dickinsonia*, and the light orange represents the small size class. See electronic supplementary material, figure S3 for a high resolution image of the KS surface.

Khatyspyt Formation records a relatively narrow basin with steep slopes developed in a marine ramp setting (electronic supplementary material, figure S2). Sedimentological observations (e.g. turbiditic nature of the limestones; evidence of strong unidirectional flows; intraclasts originating from outside of the Khatyspyt depositional basin) suggest the Khatyspyt Formation was deposited within a starved intracratonic rift, beyond the flexure slope break [69–72]. The lack of any evidence of wave reworking within the entire Khatyspyt Formation and geochemical evidence of stratification and anoxia [73], with episodic anoxia, corroborate a deep-water interpretation of the Khatyspyt depositional environment. A positive $\delta^{13}C_{carb}$ excursion in the Khatyspyt Formation has been correlated with an excursion of similar magnitude in the less than 550 Ma Gaojiashan Member of the Dengying Formation, South China [72]. Strontium isotope ratios ($^{87}Sr/^{86}Sr$) in the Khatyspyt Formation are consistently *ca* 0.7080 [72,73], a value approaching some of the ratios seen in the Gaojiashan Member [74], so this correlation seems plausible. Surface KH2 remains in the field, and surface KH1 was destroyed by excavating surface KH2. Specimens from surface KH1 reside in Trofimuk Institute of Petroleum Geology and Geophysics, collection number 913 (specimen numbers: 0607/2009-3, 0607/2009-6, 0607/2009-7, 0607/2009-17, 0607/2009-18).

1.3. Data collection

Spatial data were collected from the surfaces using different methods depending on the physical properties of the bedding plane (table 1). The WS-A, KH1, KH2 surfaces were mapped in the field (WS-A in 2017, KH1 in 2006 and 2009, and KH2 in 2018) onto millimetre graph paper (figure 2). First, the coordinates of the edge of the rock surface were recorded, then the coordinates, orientation and dimensions of each specimen were measured and plotted onto the paper. For DS, a bedding surface of 9 m² was excavated over the course of two years (2017–2018). The surface was photo-mapped, with photographs taken under an artificial light source at night. The intersection between maximum length (L) and maximum width (W) of each specimen was taken to be the absolute position of the organism, with measurements obtained from digital photographs using Adobe Photoshop CC software and Apple Script Editor (figure 2).

The KS surface was excavated in July 2004, and is a laterally discontinuous transect consisting of four slabs of variable size, ranging from 0.6 × 0.4 m to 1.6 × 1.0 m. The relative positions of the slabs within the transect were mapped *in situ* on an excavated terrace. A separate block originating from the same horizon was found in float close to the transect. Following reassembly, the taxonomic identity, positions, orientations and

shapes of the fossils were mapped at millimetre scale (figure 2). For the FUN4 and FUN5 surfaces, photogrammetric maps of the bedding surfaces were made, with lens edge effects corrected using RawTherapee (v. 2.4.1; figure 2). For all mapped palaeocommunities, fossil identification, position and dimensions (e.g. disc width, disc length, stem length, stem width, frond length and frond width) were digitized in Inkscape 0.92.3 on a two-dimensional projection of the dataset, resulting in a two-dimensional vector map for each palaeocommunity (figure 2). Only taxa that had sufficient abundance (greater than five specimens) for spatial analyses were used in this study, and these were grouped within one of six taxonomic groups: *Aspidella*, *Dickinsonia*, *Funisia*, *Kimberella*, *Orbisiana* and the trace fossil *Kimberichnus*. *Aspidella* is considered a form taxon here, in line with previous studies [65,75], and may represent multiple different types of organism, such as the holdfasts of frondose taxa. We also note that on FUN4 and FUN5, *Funisia* fossils are represented only by their holdfast 'buds', rather than by the complete *Funisia* tubular organism [76]. A group consisting of all the sessile taxa on the KS surface was also assessed, since abundance was not sufficient to include all taxa individually. Taxa were excluded from analyses if there were fewer than five specimens on the surface, because low-abundance taxa would fall below the threshold for which results would be statistically meaningful.

2. Methods

2.1. Bias analyses

For each surface, we first investigated erosional biases by testing to see if fossil density is correlated with sources of modern erosion, such as distance of the surface from the ground, or from a water source [18,71]. Since the preserved palaeo-communities are a sub-sample of the communities alive at the time, we would not expect specimen densities to correlate with modern bedding-plane features unless these features were affecting the fossil distributions. We tested for tectonic deformation by inspecting specimen and bedding-plane deformation [18,71]. If these factors were found to have significantly affected specimen density distributions, the erosion and/or deformation were taken into account when performing later analyses (cf. [23]), with heavily eroded sections of the bedding planes excluded from analyses. The influence of tectonic deformation was only observed on the DS surface, so retrodeformation techniques [18,25] were not applied to the spatial maps of WS-A, KH1, KH2, KS, FUN4 and FUN5 surfaces. Where possible (WS-A, KH1 and KH2 surfaces), the area near the outcrops was investigated, and no independent evidence of tectonic deformation was found. The holdfast discs on surfaces KS, FUN4 and FUN5 did not show any evidence of tectonic deformation. The DS surface showed signs of deformation in the form of consistent variation in specimen length to width ratios along a presumed axis of deformation. The *fitModel* function from the *mosaic* package in R [72] was used to find the best-fit values for the direction and strength of deformation using the assumption that *Dickinsonia* had a consistent length to width ratio during its ontogeny [40,77,78], though note [79], and the spatial map was accordingly retrodeformed (cf. [18,23,25]).

2.2. Spatial analyses

Initial data exploration, inhomogeneous Poisson modelling and segregation tests were performed in R [75] using the package *spatstat* [80,81]. Programita software was used to obtain distance measurements and to perform aggregation model fitting (described in detail in references [45,49,80,82–85]).

Univariate and bivariate pair correlation functions (PCFs) were calculated from assemblage population densities using a grid of $1 \text{ cm} \times 1 \text{ cm}$ cells on all surfaces except DS, where a $10 \text{ cm} \times 10 \text{ cm}$ cell size was used to correspond to the larger overall mapped area. To minimize noise, a 3 cell smoothing was calculated dependent on specimen abundance, which was applied to the PCF. To test whether the PCF exhibited complete spatial randomness (CSR), 999 simulations were run for each univariate and bivariate distribution, with the 49 highest and 49 lowest values removed. CSR was modelled by a Poisson model on a homogeneous background where the PCF = 1, and the fit of the fossil data to CSR was assessed using Diggle's goodness-of-fit test. Owing to non-independence of spatial data, Monte Carlo generated simulation envelopes cannot be interpreted as confidence intervals. If the observed data fell below the Monte Carlo simulations, the bivariate distribution was interpreted to be segregated; above the Monte Carlo simulations, the bivariate distribution was interpreted to be aggregated.

If a taxon was not randomly distributed on a homogeneous background and was aggregated, the random model on a heterogeneous background was tested by creating a heterogeneous background from the density map of the taxon under consideration. This density map was defined by a circle of radius R over which the density was averaged throughout the sample area. Density maps were formed using estimators within the range of $0.1 \text{ m} < R < 1 \text{ m}$, with R corresponding to the best-fit model used. If excursions outside the simulation envelopes for both homogeneous and heterogeneous Poisson models remained, then Thomas cluster models were fitted to the data as follows.

1. The PCF and L-function [86] of the observed data were found. Both measures were calculated to ensure that the best-fit model is not optimized towards only one distance measure, and thus encapsulates all spatial characteristics.
2. Best-fit Thomas cluster processes [87] were fitted to the two functions where PCF > 1. The best-fit lines were not fitted to fluctuations around the random line of PCF = 1 in order to aid good fit about the actual aggregations, and to limit fitting of the model about random fluctuations. Programita used the minimal contrast method to find the best-fit model.
3. If the model did not describe the observed data well, the lines were re-fitted using just the PCF. If that fit was also poor, then only the L-function was used.
4. Ninety-nine simulations of this model were generated to create simulation envelopes, and the fit checked using the O-ring statistic [82].
5. In order to assess how well the model fit the observed data, the goodness-of-fit (p_d) was calculated over the model range [85]. A $p_d = 0$ indicates no model fit, and $p_d = 1$ indicates a perfect model fit. Very small-scale segregations (of the order of specimen diameter) were not included in the model fitting, since they likely represent the finite size of the specimens, and a lack of specimen overlap.
6. If there were no excursions outside the simulation envelope and the p_d-value was high, then a univariate homogeneous Thomas cluster model was interpreted as the best model.

For any univariate distributions exhibiting CSR, the size-classes of each taxon were calculated and the univariate PCFs of the smallest size classes and largest size classes were plotted, with 999 Monte Carlo simulations of a complete spatially random distribution and segregation tests performed. The most objective way to resolve the number and range of size classes in a population is by fitting height-frequency distribution data to various models, followed by comparison of (logarithmically scaled) Bayesian information criterion (BIC) values [85], which we performed in R using the package MCLUST [88]. The number of populations identified was then used to define the most

Table 2. Goodness-of-fit tests for spatial analyses. For the inhomogeneous point processes (HP and ITC), the moving window radius is 0.5 m, using the same taxon density as the taxon being modelled. $p_d = 1$ corresponds to a perfect fit of the model to the data, while $p_d = 0$ corresponds to no fit. Where observed data did not fall outside CSR Monte Carlo simulation envelopes, no further analyses were performed, which is indicated by n.a. CSR: complete spatial randomness; HP: heterogeneous Poisson model; TC: Thomas cluster model; DTC: double Thomas cluster; ITC: inhomogeneous Thomas cluster model. N is the number of specimens mapped. Note that for the mobile taxa *Dickinsonia* and *Kimberella*, and presumed trace fossils formed by mobile taxa (*Kimberichnus*), the observed spatial pattern will also be defined by their behaviour, and so the inference of process from pattern is not as straightforward (see discussion in the main text). The p_d-value of the best-fit model is given in italics.

surface	taxon	N	CSR	HP	TC	DTC	ITC
				p_d values			
WS-A	*Aspidella*	40	0.019	*0.796*	0.504	0.2759	0.425
KH1	*Aspidella*	204	0.001	0.001	0.648	*0.883*	0.313
KH2	*Aspidella*	81	0.001	0.001	0.576	*0.932*	0.001
FUN4	*Funisia*	290	0.001	*0.9570*	0.6340	n.a.	0.245
FUN5	*Funisia*	482	0.001	*0.9080*	0.1320	n.a.	0.218
DS	*Dickinsonia*	62	*0.857*	0.022	0.025	n.a.	0.019
	Dickinsonia small	48	0.128	*0.978*	0.143	n.a.	0.158
	Dickinsonia large	14	0.388	*0.446*	0.409	n.a.	0.434
KS	all	80	*0.858*	0.381	0.328	n.a.	0.380
	all sessile	44	0.033	*0.956*	0.770	n.a.	0.761
	Kimberella	18	0.001	*0.837*	0.491	n.a.	0.103
	Orbisiana	16	0.325	*0.332*	0.326	n.a.	0.288
	Kimberichnus	6	*0.566*	n.a.	n.a.	n.a.	n.a.
	bivariate *Kimberella – Kimberichnus*	24	*0.028*	n.a.	n.a.	n.a.	n.a.

appropriate size classes. A BIC value difference of greater than 10 corresponds to a 'decisive' rejection of the hypothesis that two models are the same, whereas values less than 6 indicate only weakly rejected similarity of the models [88–92]. Once defined, the PCFs for each size class were calculated.

Bivariate analyses were performed on the KS surface (the only studied surface with multiple abundant taxa/taxon groups) between *Kimberella—Orbisiana*, *Kimberella—Kimberichnus* and *Orbisiana—Kimberichnus*. For each 'taxon' pair, the bivariate PCF was calculated, and then compared to CSR using Monte Carlo simulations and Diggle's goodness-of-fit test.

3. Results

Across the seven palaeocommunities, *Dickinsonia* on the DS surface was the only taxon that exhibited CSR (table 2). There were five univariate distributions exhibiting aggregated spatial distributions (Sessile Taxa on KS, *Funisia* on FUN4 and FUN5, *Aspidella* on KH1 and KH2), and two univariate (*Aspidella* on WS-A and large *Dickinsonia* on DS) and one bivariate (*Kimberella* and *Kimberichnus* on KS) segregated spatial distributions (figure 3, table 2). The *Aspidella* aggregations from KH1 and KH2 were best modelled by the same DTC process ($p_d^{kh1} = 0.883$, $p_d^{k21} = 0.932$, figure 3*g*,*h*; table 2), which consisted of large clusters of 20.96 cm diameter containing smaller clusters with a mean of six specimens within a cluster of 7.34 cm in diameter (figure 3*g*,*h* [93]). These results indicate that the non-random spatial distributions were most likely due to two generations of reproduction, cf. [44], and do not represent a significant interaction or association with local habitat variations. This result is consistent with previous work on

older (approx. 565 Ma) deep-water communities that also show a strong non-environmentally influenced signal [23]. In contrast, the *Aspidella* from the WS-A surface show significant segregation and are best-modelled by a heterogeneous Poisson process ($p_d^{WS-A} = 0.796$, figure 3*f*, table 2). This is consistent with small-scale intra-specific competition in a resource-limited environment [94]. *Funisia* from FUN4 and FUN5 had aggregations that are best-modelled by heterogeneous Poisson processes ($p_d^{Fun4} = 0.9570$, $p_d^{Fun5} = 0.9080$, figure 3*d*,*e*; table 2), which are interpreted to indicate significant habitat associations with the local environment.

The KS community is notably different in species composition from deep-water communities because it contains mobile organisms such as *Kimberella* and *Yorgia* [95–98] as well as putative trace fossils such as *Kimberichnus* (thought to be produced by the grazing activity of *Kimberella* specimens) [99]. We found that the KS community exhibits CSR, which suggests that any taxon-specific univariate distributions are likely to be biological/ecological in origin, rather than resulting from a taphonomic bias ($p_d^{KS}All = 0.858$, table 2, [23]). In contrast, when all the sessile taxa were grouped together they exhibited a significant aggregation (table 2), which was best-modelled by a heterogeneous Poisson process ($p_d^{KS}Sessile = 0.956$, table 2). *Kimberella* exhibits a significant aggregation under spatial scales of 20 cm ($p_d^{KS}Kimberella = 0.001$ for CSR model, figure 3*a*), with Thomas cluster and heterogeneous Poisson models fitting the data well, suggesting that behavioural factors may also influence *Kimberella* spatial patterns. The *Kimberichnus* PCF spatial distribution has a CSR distribution (figure 3*b*, $p_d^{KS} Kimberichnus = 0.566$, table 2). Furthermore, the bivariate analyses between *Kimberella* and *Kimberichnus* show a significant
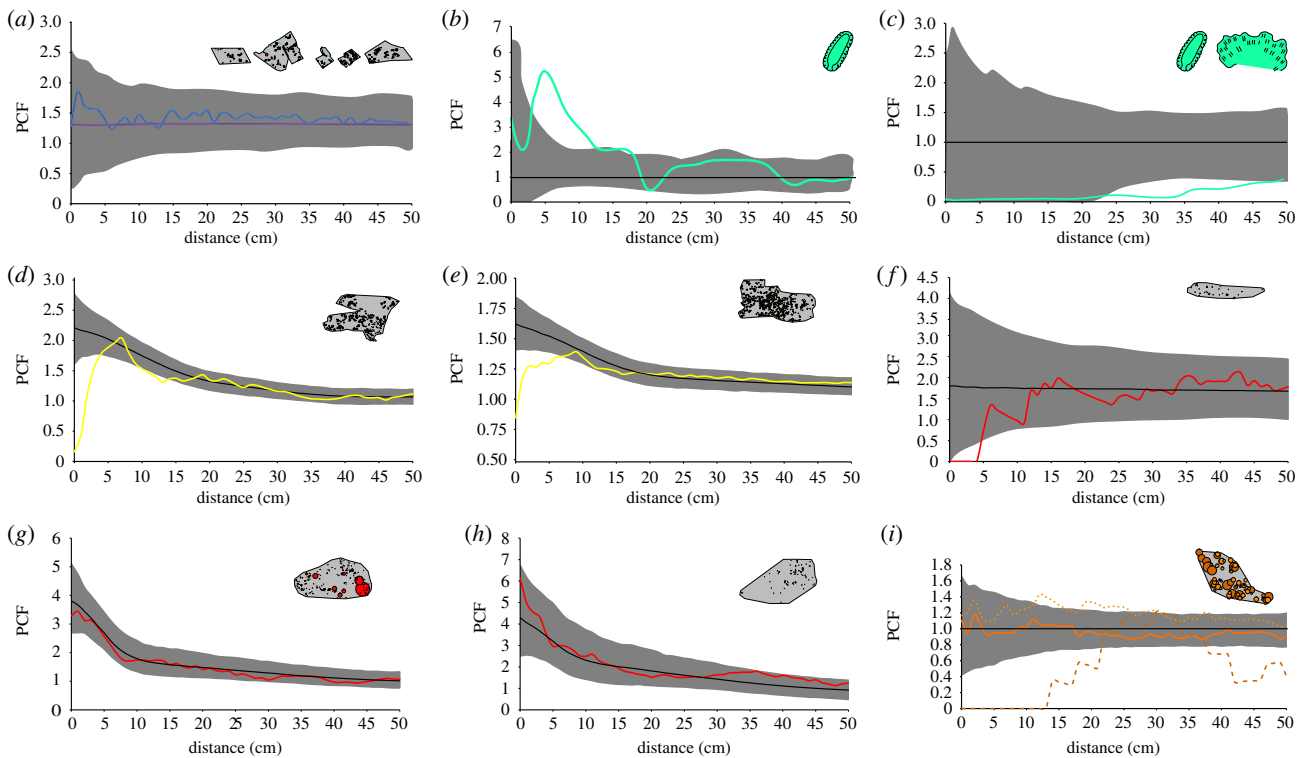
Figure 3. Pair correlation functions describing the spatial distributions of the seven studied palaeocommunities. The coloured lines are the observed data and black lines represent best-fit models (either CSR or heterogeneous Poisson). The grey area is the simulation envelope for 999 Monte Carlo simulations. The x-axis is the inter-point distance between organisms in centimetres. On the y-axis, PCF = 1 indicates complete spatial randomness (CSR), less than 1 indicates segregation, and greater than 1 indicates aggregation. (a) The KS surfaces showing sessile specimens with the black-line showing the best-fit heterogeneous Poisson model. (b) KS univariate *Kimberella*. (c) KS bivariate *Kimberella – Kimberichnus* with the CSR model shown. (d) FUN4, and (e) FUN5 surfaces showing the *Funisia* distributions with the best-fit heterogeneous Poisson model. *Aspidella* from (f) WS-A, (g) KH1 and (h) KH2 surfaces with their best-fit heterogeneous Poisson models. (i) *Dickinsonia* from DS with the solid line showing the whole population, dotted line the juveniles, and dashed line the adults, with the CSR model shown.

segregation ($p_d^{KS}{}_{\text{KimKim}^b} = 0.028$, figure 3c), which could reflect the *Kimberella* organisms avoiding patches of the surface that had already been grazed.

The *Dickinsonia* population from DS exhibited a CSR PCF distribution (figure 3i, $p_d = 0.857$). Previous analysis of the population of *Dickinsonia* from DS showed two cohorts in the size distribution [93]. The two cohorts exhibited different PCF spatial behaviour, with the small specimens aggregating with a best-fit heterogeneous Poisson model (figure 3i, $p_d^{\text{small}} = 0.978$) and the large specimens exhibiting segregation (figure 3i).

3.1. Interpreting the spatial distributions of mobile organisms

For mobile organisms, inferring the underlying process behind the observed spatial distributions is imprecise, since their spatial patterns also incorporate contributions from their behaviour. Modern animals move primarily to find resources, mates, microhabitats and/or escape predators or detrimental environmental conditions. There is no direct evidence of predators in the Ediacaran, unless perforations in the terminal Ediacaran calcareous tubes of *Cloudina* could be referred to as borings [100]. The lack of resolution of reproductive strategies of *Dickinsonia* means that we cannot predict resultant spatial patterns, and thus cannot definitively rule reproductive processes out as a source of spatial patterning. Such reproduction may or may not include necessity for close proximity and/or broadcast spawning cf. the majority of extant benthic organisms [101]. However, reproductive processes are considered an unlikely

explanation for the observed spatial patterns because the *Dickinsonia* do not aggregate as might be expected in a mating event, as demonstrated by the largest size class in the studied *Dickinsonia* population segregation (figure 3c, table 2). Furthermore, broadcast spawning does not require the two mating organisms to be within the spatial scale (less than 40 cm) found on the DS surface. We cannot determine whether the large *Dickinsonia* are reacting to the mortality event that killed and preserved them; however, this would not explain the complex interplay between aggregated and segregated behaviours. Therefore, for this *Dickinsonia* population, the search for resources and/or microhabitats is considered the most plausible explanation, particularly since this hypothesis is further supported by their spatial patterns. Aggregated–segregated PCF patterns such as those seen in our *Dickinsonia* population are common in extant sessile organisms where juveniles are initially aggregated on preferred habitats but then begin to compete with each other as they require greater resources, leading to thinning or segregation among adult populations. While it is not possible to confirm the underlying mechanism for the distribution of the studied *Dickinsonia* population, given the preceding points we consider it most likely to be motivated by associations with preferential habitat for food and/or resources. Further analyses of other *Dickinsonia* surfaces would enable more robust conclusions to be reached.

3.2. Time averaging

The preservation of time-averaged communities has the potential to bias our analyses (see [21,25]). In Avalonian
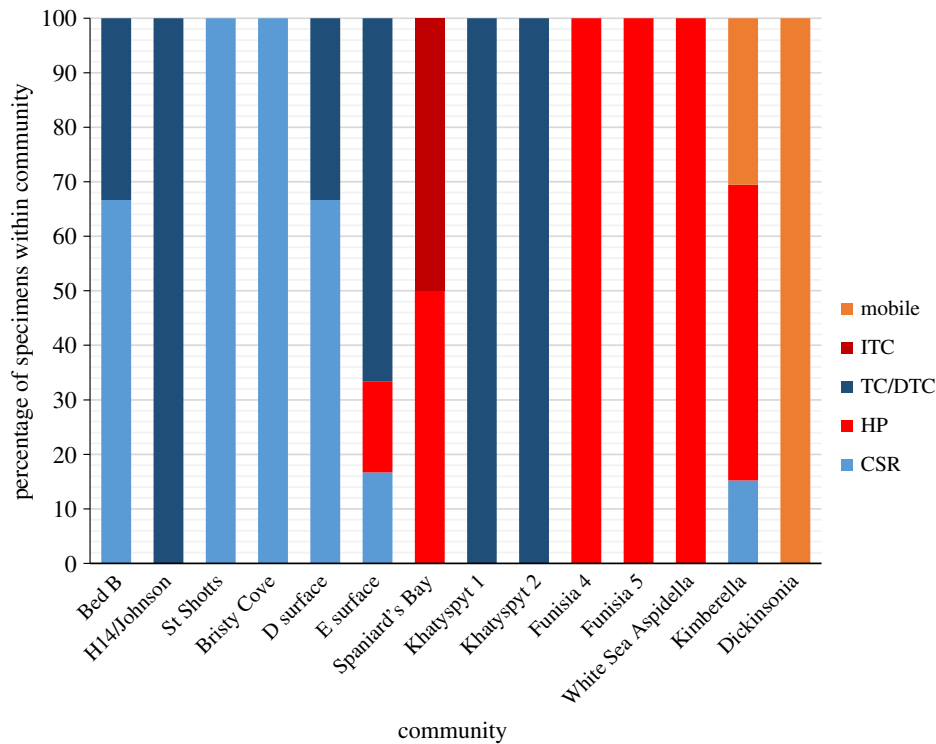
Figure 4. Proportion of best-fit univariate models by surface, adapted from [23]. The percentage of studied body-fossil specimens within the community with univariate spatial distributions that are best described by CSR, HP, TC (or DTC) and ITC models. CSR and TC are considered random or dispersal (neutral) models and are shown in blue. HP and ITC are local environmentally driven (niche) models, shown in red. Mobile taxa are shown in orange, and inferred to be environmentally-driven. Data for surfaces Bed B to Spaniard's Bay from ref. [23].

communities, taphomorphs interpreted to record the decaying remains of organisms are identified by their poor preservational fidelity, irregular morphologies, and often high topographic relief [102]. This interpretation is consistent with data suggesting that the spatial interactions of some taphomorph populations mirror those of other taxa they are considered to be derived from [21]. Taphomorphs are considered unlikely to have imparted a significant signal on these studied surfaces, since we did not observe ivesheadiomorph-type forms, and there is a consistent level of preservational detail among fossil communities.

Funisia communities tend to have very similar diameters for the holdfasts, which suggests single colonization events [76]. Different reproductive events can be distinguished by population analyses of size-distributions [103], with each reproductive event identified as a statistically significant cohort within the size-distribution [88]. Surfaces FUN4 and FUN5 both exhibit populations with two cohorts (electronic supplementary material, figure S4), most likely indicating two reproductive/colonization events. The best-fit models for each of these surfaces are heterogeneous Poisson models (figure 3, table 2), with very high goodness-of-fit values ($p_d > 0.90$) reflecting a single model for each surface. Therefore, cohorts of *Funisia* specimens on each of the studied surfaces were affected by the same underlying environmental heterogeneity, so most likely were contemporaneous.

4. Discussion

The spatial distributions of five of the seven studied palaeocommunities provide compelling evidence that their local environment had a significant influence on those communities (figure 3, table 2). In modern settings, habitat associations form when a patchy resource provides heterogeneously distributed preferential conditions for the establishment and growth of sessile taxa, and/or feeding 'hotspots' for mobile taxa. The presence of inferred habitat interactions within our palaeocommunities showed a significant correlation with the environmental setting (Kruskal–Wallis test, $p = 0.049$), with all five palaeocommunities with strong habitat interactions derived from nearshore depositional environments. The two communities that were seemingly not strongly influenced by their local habitat are from offshore, deeper-water facies (table 2). These results are consistent with previous work, which found that for seven independent deep-marine (slope and basin) Ediacaran palaeocommunities from Newfoundland and Charnwood Forest, only one was dominated by associations of taxa with local habitat heterogeneities [21–23] (Kruskal–Wallis test of all data, $p = 0.021$; figure 4).

Untangling environmental from evolutionary trends in the Ediacaran has been hampered by a limited overlap between temporal intervals and environmental settings [1,17]. The palaeocommunities in this study derive from successions containing a variety of lithologies (tuff, coarse sandstone, mixed siltstone, limestone) and reflecting different palaeogeographic positions [17,63,64,76,104–106]. We find no significant direct correlations between these factors and the relative importance of habitat heterogeneities on the studied surfaces ($p \gg 0.1$; figure 3, table 2). The palaeocommunities that are not influenced by local habitat heterogeneities (KH1 and KH2) are hosted within carbonate successions [106], making them distinct from the siliciclastically hosted palaeocommunities on the KS, WS-A, FUN4, FUN5 and DS surfaces, or in previous work [21–23]. However, the Khatyspyt surfaces behave ecologically in the same way to Avalonian palaeocommunities

derived from siliciclastic successions of similar depths [21–23], suggesting that lithology alone may not be responsible for the KH1 and KH2 surfaces displaying differing results. Therefore, two possible factors remain that may explain the differences in community dynamics found here. The differences could reflect evolutionary trends, and it is true that the oldest studied palaeocommunities show limited habitat influence [21–23] when compared to the younger palaeocommunities documented in this study (figure 4). Unfortunately, the lack of fine-scale dating across these palaeocommunities precludes detailed fine-scale regression to assess whether the Khatyspyt palaeocommunities are an outlier to this apparent trend, or this trend merely reflects the biases of the available data. Alternatively, the differences could be due to the environmental setting. We have shown that Ediacaran environmental setting has a significant influence on community dynamics ($p = 0.021$), with shallower water palaeocommunities significantly influenced by habitat heterogeneities, in contrast to the deeper water palaeocommunities (figure 3, table 2; [21–23]). This result does not preclude a simultaneous temporal influence, but given our dataset we are limited to only assessing the broad environmental factor. Our dataset also precludes a more detailed analysis of the relationship between community ecologies and different environmental facies, hence the focus on broad signals (shallow/deep). The surfaces included in this study consist of a small proportion of the known Ediacaran palaeocommunities, and were frequently depauperate in taxonomic diversity, so in order to fully corroborate the proposed hypotheses, analysis of more surfaces from a wider range of global localities is required.

While SPPA have only been applied to a small proportion of the known in situ Ediacaran palaeocommunities (17 studied surfaces to date), there is a notable correspondence between the importance of habitat heterogeneities to community ecology and assemblage diversity. In this study, the palaeocommunities exhibiting significant influence from local habitat heterogeneities belong to the diverse White Sea assemblage, in contrast to the previous work on Avalonian palaeocommunities [21–23], which are not significantly influenced by such heterogeneities. The relationship between environmental spatial heterogeneities and extant species richness is well established, with habitat variations enabling species to coexist through the creation of different niches [107]. This relationship extends to modern deep-sea benthic communities, where these heterogeneities have been shown to provide a mechanism for diversification over large spatial scales, such as between canyons, trenches and seamounts [108,109], on the centimetre to metre scale [110], and through microhabitats [42].

In the modern oceans, three relevant mechanisms increase habitat heterogeneity, and they involve an increase in both substrate heterogeneity and variation in differentiated particulate organic carbon (POC) and matter (POM) within the water column. First, metazoan mat grazing creates substrate heterogeneity in microbial substrates via the formation of depleted and non-depleted patches [111]. Secondly, this grazing induces creation of different-sized detrital particles in the form of differential-sized faecal pellets and fragments of non-consumed food within the water-column, leading to water-column heterogeneity [112]. Differential POC and POM create new food sources and therefore new niches, and have been shown to increase the biodiversity of sessile benthic communities [113–115]. Thirdly, the main source of deep-sea habitat heterogeneity is small-scale variation

due to differentiated particle influx, with diurnal vertical migration of mesozooplankton and macrofauna contributing up to approximately 50% of POC to the modern deep-sea via faecal pellets [116–118], with the remaining approximately 50% transported from shallow to deep-water via oceanic currents [119]. Taken together, these modern processes describe how grazing in the shallow waters contributes to habitat heterogeneity in deep-water communities in the form of differentiated POC/POM.

Tentatively, we propose that the ecological differentiation observed between Ediacaran nearshore and offshore communities may evidence the late Ediacaran development of a similar chain of evolutionary diversification. This chain started in shallow water communities, with the creation of habitat patchiness by mobile Ediacaran organisms, which then led to a feedback of increasing diversification that ultimately expanded into the deep-sea. This hypothesized feedback could have promoted diversification through the latest Ediacaran by increasing heterogeneity. First, our data suggest that once grazing had occurred, organisms such as Kimberella may have avoided pre-grazed patches (figure 3c, table 2), with this selective grazing accelerating further creation of mat heterogeneity and water-column heterogeneity via differentiated POC (cf. [110,111]). Secondly, this differentiated POC and POM would have been transported to deeper settings via oceanic currents [119]. Diurnal vertical migration was likely absent [6] in the Ediacaran, because while a planktonic/larval stage for Ediacaran organisms has been predicted on the basis of their likely waterborne dispersal strategies [25,103], there is presently no direct evidence of non-larval, planktotrophic zooplankton until the onset of the Cambrian. In the absence of planktotrophic zooplankton and widespread pelagic macrofauna, the Ediacaran POC flux may have been either larger, due to lack of consumption of phytoplankton in the shallow water, or smaller, due to a lack of mixing by diurnal vertical migration of the plankton [6], and this cannot yet be determined. Prior to grazers and detritivores, the POC/POM flux would have been dominated by relatively homogeneous phytodetritus. The evolution of grazers would have facilitated a shift towards size-differentiated POC/POM, potentially increasing the heterogeneity of the deep-sea habitat via water-column heterogenization [113–115], and so providing a mechanism for deep-marine diversification.

Budd & Jensen [12] introduced the Savannah hypothesis to explain early animal diversification, whereby early bilaterian diversification was driven by small-scale variations in local habitat, primarily caused by the spatial distributions of sessile organisms. They argue that it was the drive to find these heterogeneous distributed resources that led to novel evolutionary innovations such as mobility. Our results demonstrate that at least some of the early animal communities that contain mobile organisms were influenced by habitat variations, but the limited number of studied surfaces means that we cannot test whether the observed patchiness results from the spatial distributions of the sessile organisms, or another source. However, we do describe a mechanism that links early animal diversification and benthic habitat patchiness prior to the evolution of predators and widespread pelagic organisms. We show that taxa such as Kimberella had a segregated distribution with trace fossils considered to be their grazing traces [97], suggesting that they may have been capable of avoiding non-preferred areas (possibly already consumed patches), revealing adaptation of behaviour when interacting with
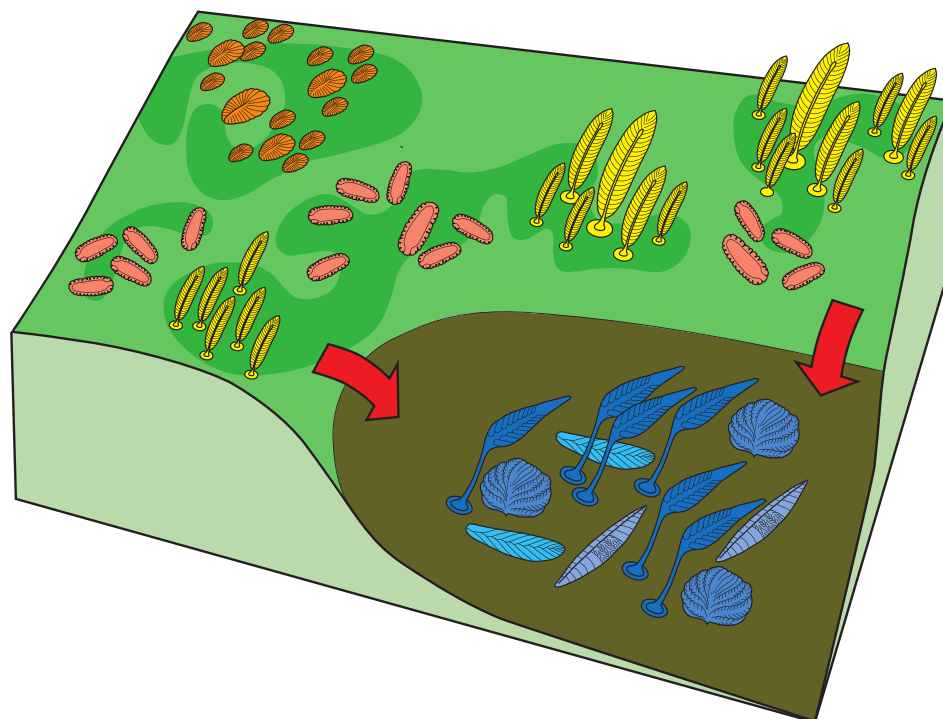
Figure 5. Schematic diagram showing variation of heterogeneities within different environmental settings. Shallow water communities are significantly influenced by habitat heterogeneities. Grazing within these shallow waters further increases substrate heterogeneity, potentially increasing diversification. Furthermore, this grazing increases deep-water heterogeneity through the creation and influx of different sized particulate organic matter from the shallows, offering a potential mechanism via which to drive deep-marine diversification.

these patches. This adaptation theoretically has the capacity to drive further diversification, initially dependent on the environmental setting, starting in shallow water depositional environments, and then, over time, moving into deeper water, but currently available global fossil assemblages limit the testing of this prediction. If this hypothesis is correct, we would expect deep-water assemblages to diversify during the terminal Ediacaran and into the Cambrian. Our results therefore provide tentative support for the Savannah hypothesis, suggesting that this late Ediacaran taxonomic diversification was a benthic event, which could have facilitated a chain of diversification by promoting marine habitat heterogeneities (figure 5).

5. Conclusion

We present evidence to suggest that the influence of local habitat on Ediacaran organisms is significantly correlated with broad-scale environmental setting. The relationship of Ediacaran communities to habitat-dependent interactions is correlated with Ediacaran assemblage diversity, with communities from the more diverse White Sea assemblage showing significant habitat associations and interactions in contrast to relatively habitat insensitive deep-sea Avalonian assemblages. We suggest that the presence of shallow-water grazers could have created further habitat heterogeneity first in shallow-water settings, and ultimately in deep-waters, via the heterogenization of the shallow-water substrate and the introduction of variable size particulate matter to the deep-sea. These results demonstrate both the utility of SPPA approaches for investigating the early diversification of metazoans, and the importance of local environmental patchiness to the

diversification of early animals, and they are consistent with the hypothesis that the early diversification of metazoans was a benthic event driven by responses to habitat patchiness.

References

1. Wood R, Liu AG, Bowyer F, Wilby PR, Dunn FS, Kenchington CG Hoyal, Cuthill JF, Mitchell EG, Penny A. 2019 Integrated records of environmental change and evolution challenge the Cambrian Explosion. *Nat. Ecol. Evol.* **3**, 528–538. (doi:10.1038/s41559-019-0821-6)

2. Xiao S, Laflamme M. 2009 On the eve of animal radiation: phylogeny, ecology and evolution of the Ediacara biota. *Trends Ecol. Evol.* **24**, 31–40. (doi:10.1016/j.tree.2008.07.015)

3. Erwin DH, Laflamme M, Tweedt SM, Sperling EA, Pisani D, Peterson KJ. 2011 The Cambrian conundrum: early divergence and later ecological success in the early history of animals. *Science* **334**, 1091–1097. (doi:10.1126/science.1206375)

4. Lenton TM, Boyle RA, Poulton SW, Shields-Zhou GA, Butterfield NJ. 2014 Co-evolution of eukaryotes and ocean oxygenation in the Neoproterozoic Era. *Nat. Geosci.* **7**, 257–265. (doi:10.1038/ngeo2108)

5. Butterfield NJ. 2009 Macroevolutionary turnover through the Ediacaran transition: ecological and biogeochemical implications. *Geol. Soc. Lond. Spec. Publ.* **326**, 55–66. (doi:10.1144/SP326.3)

6. Butterfield NJ. 2018 Oxygen, animals and aquatic bioturbation: an updated account. *Geobiology* **16**, 3–16. (doi:10.1111/gbi.12267)

7. Sperling EA, Frieder CA, Raman AV, Girguis PR, Levin LA, Knoll AH. 2013 Oxygen, ecology, and the Cambrian radiation of animals. *Proc. Natl Acad. Sci. USA* **110**, 13 446–13 451. (doi:10.1073/pnas.1312778110)

8. Lenton TM, Daines SJ. 2018 The effects of marine eukaryote evolution on phosphorus, carbon and oxygen cycling across the Proterozoic–Phanerozoic transition. *Emerg. Top. Life Sci.* **2**, 267–278. (doi:10.1042/ETLS20170156)

9. Wood R, Erwin DH. 2018 Innovation not recovery: dynamic redox promotes metazoan radiations. *Biol. Rev.* **93**, 863–873. (doi:10.1111/brv.12375)

10. Butterfield NJ. 2011 Animals and the invention of the Phanerozoic Earth system. *Trends Ecol. Evol.* **26**, 81–87. (doi:10.1016/j.tree.2010.11.012)

11. Mángano MG, Buatois LA. 2014 Decoupling of body-plan diversification and ecological structuring during the Ediacaran–Cambrian transition: evolutionary and geobiological feedbacks. *Proc. R. Soc. B* **281**, 20140038. (doi:10.1098/rspb.2014.0038)

12. Budd GE, Jensen S. 2017 The origin of the animals and a 'Savannah' hypothesis for early bilaterian evolution. *Biol. Rev.* **92**, 446–473. (doi:10.1111/brv.12239)

13. Muscente AD, Boag TH, Bykova N, Schiffbauer JD. 2018 Environmental disturbance, resource availability, and biologic turnover at the dawn of animal life. *Earth Sci. Rev.* **177**, 248–264. (doi:10.1016/j.earscirev.2017.11.019)

14. McPeek MA. 2017 The ecological dynamics of natural selection: traits and the coevolution of community structure. *Am. Nat.* **189**, E91–117. (doi:10.1086/691101)

15. Waggoner B. 2003 The Ediacaran biotas in space and time. *Integr. Comp. Biol.* **43**, 104–113. (doi:10.1093/icb/43.1.104)

16. Grazhdankin D. 2004 Patterns of distribution in the Ediacaran biotas: facies versus biogeography and evolution. *Paleobiology* **30**, 203–221. (doi:10.1666/0094-8373(2004)030<0203:PODITE>2.0.CO;2)

17. Boag TH, Darroch SAF, Laflamme M. 2016 Ediacaran distributions in space and time: testing assemblage concepts of earliest macroscopic body fossils. *Paleobiology* **42**, 574–594. (doi:10.1017/pab.2016.20)

18. Wood DA, Dalrymple RW, Narbonne GM, Gehling JG, Clapham ME. 2003 Paleoenvironmental analysis of the late Neoproterozoic Mistaken Point and Trepassey formations, southeastern Newfoundland. *Can. J. Earth Sci.* **40**, 1375–1391. (doi:10.1139/e03-048)

19. Gehling JG, Droser ML. 2013 How well do fossil assemblages of the Ediacara Biota tell time? *Geology* **41**, 447–450. (doi:10.1130/G33881.1)

20. Clapham ME, Narbonne GM, Gehling JG. 2003 Paleoecology of the oldest known animal communities: Ediacaran assemblages at Mistaken Point, Newfoundland. *Paleobiology* **29**, 527–544. (doi:10.1666/0094-8373(2003)029<0527:POTOKA>2.0.CO;2)

21. Mitchell EG, Butterfield NJ. 2018 Spatial analyses of Ediacaran communities at Mistaken Point. *Paleobiology* **44**, 40–57. (doi:10.1017/pab.2017.35)

22. Mitchell EG, Kenchington CG. 2018 The utility of height for the Ediacaran organisms of Mistaken Point. *Nat. Ecol. Evol.* **2**, 1218–1222. (doi:10.1038/s41559-018-0591-6)

23. Mitchell EG, Harris S, Kenchington CG, Vixseboxse P, Roberts L, Clark C, Dennis A, Liu AG, Wilby PR. 2019 The importance of neutral over niche processes in structuring Ediacaran early animal communities. *Ecol. Lett.* **22**, 2028–2038. (doi:10.1111/ele.13383)

24. Coutts FJ, Gehling JG, García-Bellido DC. 2016 How diverse were early animal communities? An example from Ediacara Conservation Park, Flinders Ranges, South Australia. *Alcheringa* **40**, 407–421. (doi:10.1080/03115518.2016.1206326)

25. Mitchell EG, Kenchington CG, Liu AG, Matthews JJ, Butterfield NJ. 2015 Reconstructing the reproductive mode of an Ediacaran macro-organism. *Nature* **524**, 343–346. (doi:10.1038/nature14646)

26. Wilby PR, Carney JN, Howe MPA. 2011 A rich Ediacaran assemblage from eastern Avalonia: evidence of early widespread diversity in the deep ocean. *Geology* **39**, 655–658. (doi:10.1130/G31890.1)

27. Narbonne GM. 2005 The Ediacara biota: Neoproterozoic origin of animals and their ecosystems. *Annu. Rev. Earth Planet. Sci.* **33**, 421–442. (doi:10.1146/annurev.earth.33.092203.122519)

28. Pu JP, Bowring SA, Ramezani J, Myrow P, Raub TD, Landing E, Mills A, Hodgin E, Macdonald FA. 2016 Dodging snowballs: geochronology of the Gaskiers glaciation and the first appearance of the Ediacaran biota. *Geology* **44**, 955–958. (doi:10.1130/G38284.1)

29. Noble SR, Condon DJ, Carney JN, Wilby PR, Pharaoh TC, Ford TD. 2015 U-Pb geochronology and global context of the Charnian Supergroup, UK: constraints on the age of key Ediacaran fossil assemblages. *Geol. Soc. Am. Bull.* **127**, 250–265. (doi:10.1130/B31013.1)

30. Bush AM, Bambach RK, Erwin DH. 2011 Ecospace utilization during the Ediacaran radiation and the Cambrian eco-explosion. In *Quantifying the evolution of early life: numerical approaches to the evaluation of fossils and ancient ecosystems* (eds M Laflamme, JD Schiffbauer, SQ Dornbos), pp. 111–133, vol. 36. New York, NY: Springer.

31. Shen B, Dong L, Xiao S, Kowalewski M. 2008 The Avalon explosion: evolution of Ediacara morphospace. *Science* **319**, 81–84. (doi:10.1126/science.1150279)

32. Liu AG, McIlroy D, Brasier MD. 2010 First evidence for locomotion in the Ediacara biota from the 565 Ma Mistaken Point Formation, Newfoundland. *Geology* **38**, 123–126. (doi:10.1130/G30368.1)

33. Gage JD, Tyler PA. 1981 Re-appraisal of age composition, growth and survivorship of the deep-sea brittle star Ophiura ljungmani from size structure in a sample time series from the Rockall Trough. *Mar. Biol.* **64**, 163–172. (doi:10.1007/BF00397105)

34. Tecchio S, Ramírez-Llodra E, Sardà F, Company JB. 2011 Biodiversity of deep-sea demersal megafauna in western and central Mediterranean basins. *Sci. Mar.* **75**, 341–350. (doi:10.3989/scimar.201175n2341)

35. Seilacher A, Grazhdankin D, Legouta A. 2003 Ediacaran biota: the dawn of animal life in the shadow of giant protists. *Paleontol. Res.* **7**, 43–54. (doi:10.2517/prpsj.7.43)

36. Droser ML, Gehling JG. 2015 The advent of animals: the view from the Ediacaran. *Proc. Natl Acad. Sci. USA* **112**, 4865–4870. (doi:10.1073/pnas.1403669112)

37. Duda J-P, Blumenberg M, Thiel V, Simon K, Zhu M, Reitner J. 2014 Geobiology of a palaeoecosystem with Ediacara-type fossils: the Shibantan Member (Dengying Formation, South China). *Precambrian Res.* **255**, 48–62. (doi:10.1016/j.precamres.2014.09.012)

38. Chen Z, Chen X, Zhou C, Yuan X, Xiao S. 2018 Late Ediacaran trackways produced by bilaterian animals with paired appendages. *Sci. Adv.* **4**, eaao6691. (doi:10.1126/sciadv.aao6691)

39. Droser ML et al. 2019 Piecing together the puzzle of the Ediacara Biota: excavation and reconstruction at the Ediacara National Heritage site Nilpena (South Australia). *Palaeogeogr. Palaeoclimatol. Palaeoecol.* **513**, 132–145. (doi:10.1016/j.palaeo.2017.09.007)

40. Reid LM, García-Bellido DC, Gehling JG. 2018 An Ediacaran opportunist? Characteristics of a juvenile *Dickinsonia costata* population from Crisp Gorge, South Australia. *J. Paleontol.* **92**, 313–322. (doi:10.1017/jpa.2017.142)

41. Finnegan S, Gehling JG, Droser ML. 2019 Unusually variable paleocommunity composition in the oldest metazoan fossil assemblages. *Paleobiology* **45**, 235–245. (doi:10.1017/pab.2019.1)

42. Kukert H, Smith CR. 1992 Disturbance, colonization and succession in a deep-sea sediment community: artificial-mound experiments. *Deep Sea Res. A* **39**, 1349–1371. (doi:10.1016/0198-0149(92)90073-3)

43. Liu AG, Kenchington CG, Mitchell EG. 2015 Remarkable insights into the paleoecology of the Avalonian Ediacaran macrobiota. *Gondwana Res.* **27**, 1355–1380. (doi:10.1016/j.gr.2014.11.002)

44. Illian DJ, Penttinen PA, Stoyan DH, Stoyan DD. 2008 *Statistical analysis and modelling of spatial point patterns*. Chichester, UK: John Wiley & Sons.

45. Wiegand T, Gunatilleke S, Gunatilleke N, Okuda T. 2007 Analyzing the spatial structure of a Sri Lankan tree species with multiple scales of clustering. *Ecology* **88**, 3088–3102. (doi:10.1890/06-1350.1)

46. Seidler TG, Plotkin JB. 2006 Seed dispersal and spatial pattern in tropical trees. *PLoS Biol.* **4**, e344. (doi:10.1371/journal.pbio.0040344)

47. Getzin S, Dean C, He F, Trofymow JA, Wiegand K, Wiegand T. 2006 Spatial patterns and competition of tree species in a Douglas-fir chronosequence on Vancouver Island. *Ecography* **29**, 671–682. (doi:10.1111/j.2006.0906-7590.04675.x)

48. Lingua E, Cherubini P, Motta R, Nola P. 2008 Spatial structure along an altitudinal gradient in the Italian central Alps suggests competition and facilitation among coniferous species. *J. Veg. Sci.* **19**, 425–436. (doi:10.3170/2008-8-18391)

49. Getzin S, Dean C, He F, Trofymow JA, Wiegand K, Wiegand T. 2008 Heterogeneity influences spatial patterns and demographics in forest stands. *J. Ecol.* **96**, 807–820. (doi:10.1111/j.1365-2745.2008.01377.x)

50. Wiegand T, Moloney KA, Moloney KA. 2013 *Handbook of spatial point-pattern analysis in ecology*, 1st edn. Boca Raton, FL, USA. Chapman and Hall/CRC.

51. Lin Y-C, Chang L-W, Yang K-C, Wang H-H, Sun I-F. 2011 Point patterns of tree distribution determined by habitat heterogeneity and dispersal limitation. *Oecologia* **165**, 175–184. (doi:10.1007/s00442-010-1718-x)

52. Diggle P, Zheng P, Durr P. 2005 Nonparametric estimation of spatial segregation in a multivariate point process: bovine tuberculosis in Cornwall, UK. *J. R. Stat. Soc. Ser. C Appl. Stat.* **54**, 645–658. (doi:10.1111/j.1467-9876.2005.05373.x)

53. Law R, Illian J, Burslem DFRP, Gratzer G, Gunatilleke CVS, Gunatilleke IA. 2009 Ecological information from spatial patterns of plants: insights from point process theory. *J. Ecol.* **97**, 616–628. (doi:10.1111/j.1365-2745.2009.01510.x)

54. Comita L, Condit R, Hubbell SP. 2007 Developmental changes in habitat associations of tropical trees. *J. Ecol.* **95**, 482–492. (doi:10.1111/j.1365-2745.2007.01229.x)

55. Mitchell EG, Kenchington CG, Harris S, Wilby PR. 2018 Revealing rangeomorph species characters using spatial analyses. *Can. J. Earth Sci.* **55**, 1262–1270. (doi:10.1139/cjes-2018-0034)

56. Grazhdankin D. 2000 The Ediacaran genus *Inaria*: a taphonomic/morphodynamic analysis. *Neues Jahrb. Geol. Palaeontol. Abh.* **216**, 1–34. (doi:10.1127/njgpa/216/2000/1)

57. Schmitz M (ed) 2012 In *The Geologic Time Scale 2012*, pp. 1045–1082. Oxford, UK: Elsevier.

58. Martin MW, Grazhdankin DV, Bowring SA, Evans DAD, Fedonkin MA, Kirschvink JL. 2000 Age of Neoproterozoic bilatarian body and trace fossils, White Sea, Russia: implications for metazoan evolution. *Science* **288**, 841–845. (doi:10.1126/science.288.5467.841)

59. Tarhan LG, Droser ML, Gehling JG, Dzaugis MP. 2017 Microbial mat sandwiches and other anactualistic sedimentary features of the Ediacara Member (Rawnsley Quartzite, South Australia): implications for interpretation of the Ediacaran sedimentary record. *Palaios* **32**, 181–194. (doi:10.2110/palo.2016.060)

60. Droser ML, Gehling JG, Dzaugis ME, Kennedy MJ, Rice D, Allen MF. 2014 A new Ediacaran fossil with a novel sediment displaced life habit. *J. Paleontol.* **88**, 145–151. (doi:10.1666/12-158)

61. Tarhan LG, Droser ML, Gehling JG, Dzaugis MP. 2015 Taphonomy and morphology of the Ediacara form genus *Aspidella*. *Precambrian Res.* **257**, 124–136. (doi:10.1016/j.precamres.2014.11.026)

62. Reid LM, Payne JL, García-Bellido DC, Jago JB. 2020 The Ediacara Member, South Australia: lithofacies and palaeoenvironments of the Ediacara biota. *Gondwana Res.* **80**, 321–334. (doi:10.1016/j.gr.2019.09.017)

63. Grazhdankin DV, Maslov A, Krupenin M, Mustill T. 2005 The Ediacaran White Sea biota in the Central Urals. *Dokl. Earth Sci.* **401A**, 382–385.

64. Grazhdankin DV, Maslov AV, Krupenin MT. 2009 Structure and depositional history of the Vendian Sylvitsa Group in the western flank of the Central Urals. *Stratigr. Geol. Correl.* **17**, 476. (doi:10.1134/S0869593809050025)

65. Bobkov NI, Kolesnikov AV, Maslov AV, Grazhdankin D. 2019 The occurrence of *Dickinsonia* in non-marine facies. *Estudios geológicos* **75**, e096. (doi:10.3989/egeol.43587.551)

66. Bobrovskiy I, Hope JM, Ivantsov A, Nettersheim BJ, Hallmann C, Brocks JJ. 2018 Ancient steroids establish the Ediacaran fossil *Dickinsonia* as one of the earliest animals. *Science* **361**, 1246–1249. (doi:10.1126/science.aat7228)

67. Fedonkin MA, Simonetta A, Ivantsov AY. 2007 New data on *Kimberella*, the Vendian mollusc-like organism (White Sea region, Russia): palaeoecological and evolutionary implications. *Geol. Soc. Lond. Spec. Publ.* **286**, 157–179. (doi:10.1144/SP286.12)

68. Kolesnikov AV, Liu AG, Danelian T, Grazhdankin DV. 2018 A reassessment of the problematic Ediacaran genus *Orbisiana* Sokolov 1976. *Precambrian Res.* **316**, 197–205. (doi:10.1016/j.precamres.2018.08.011)

69. Knoll AH, Grotzinger JP, Kaufman AJ, Kolosov P. 1995 Integrated approaches to terminal Proterozoic stratigraphy: an example from the Olenek Uplift,

northeastern Siberia. *Precambrian Res.* **73**, 251–270. (doi:10.1016/0301-9268(94)00081-2)

70. Pelechaty SM, Grotzinger JP, Kashirtsev VA, Zhernovsky VP. 1996 Chemostratigraphic and sequence stratigraphic constraints on Vendian-Cambrian basin dynamics, Northeast Siberian Craton. *J. Geol.* **104**, 543–563. (doi:10.1086/629851)

71. Nagovitsin KE, Rogov VI, Marusin VV, Karlova GA, Kolesnikov AV, Bykova NV, Grazhdankin DV. 2015 Revised Neoproterozoic and Terreneuvian stratigraphy of the Lena-Anabar Basin and north-western slope of the Olenek Uplift, Siberian Platform. *Precambrian Res.* **270**, 226–245. (doi:10.1016/j.precamres.2015.09.012)

72. Cui H, Grazhdankin DV, Xiao S, Peek S, Rogov VI, Bykova NV, Sievers NE, Liu XM, Kaufman AJ. 2016 Redox-dependent distribution of early macro-organisms: evidence from the terminal Ediacaran Khatyspyt Formation in Arctic Siberia. *Palaeogeogr. Palaeoclimatol. Palaeoecol.* **461**, 122–139. (doi:10.1016/j.palaeo.2016.08.015)

73. Vishnevskaya IA, Letnikova EF, Vetrova NI, Kochnev BB, Dril SI. 2017 Chemostratigraphy and detrital zircon geochronology of the Neoproterozoic Khorbusuonka Group, Olenek Uplift, Northeastern Siberian platform. *Gondwana Res.* **51**, 255–271. (doi:10.1016/j.gr.2017.07.010)

74. Cui H, Xiao S, Cai Y, Peek S, Plummer RE, Kaufman AJ. 2019 Sedimentology and chemostratigraphy of the terminal Ediacaran Dengying Formation at the Gaojiashan section, South China. *Geol. Mag.* **156**, 1924–1948. (doi:10.1017/S0016756819000293)

75. R Core Team. 2017 R: A Language and Environment for Statistical Computing. R Foundation for Statistical Computing, Vienna, Austria. https://www.R-project.org/.

76. Droser ML, Gehling JG. 2008 Synchronous aggregate growth in an abundant new Ediacaran tubular organism. *Science* **319**, 1660–1662. (doi:10.1126/science.1152595)

77. Evans SD, Gehling JG, Droser ML. 2019 Slime travelers: early evidence of animal mobility and feeding in an organic mat world. *Geobiology* **17**, 490–509. (doi:10.1111/gbi.12351)

78. Evans SD, Droser ML, Gehling JG. 2017 Highly regulated growth and development of the Ediacara macrofossil *Dickinsonia costata*. *PLoS ONE* **12**, e0176874. (doi:10.1371/journal.pone.0176874)

79. Evans SD, Huang W, Gehling JG, Kisailus D, Droser ML. 2019 Stretched, mangled, and torn: responses of the Ediacaran fossil *Dickinsonia* to variable forces. *Geology* **47**, 1049–1053. (doi:10.1130/G46574.1)

80. Baddeley A, Rubak E, Turner R, Rubak E, Turner R. 2015 *Spatial point patterns: methodology and applications with R*. Boca Raton, FL: Chapman and Hall/CRC.

81. Berman M. 1986 Testing for spatial association between a point process and another stochastic process. *J. R. Stat. Soc. Ser. C Appl. Stat.* **35**, 54–62.

82. Wiegand T, Moloney KA. 2004 Rings, circles, and null-models for point pattern analysis in ecology.

Oikos **104**, 209–229. (doi:10.1111/j.0030-1299.2004.12497.x)

83. Wiegand T, Kissling WD, Cipriotti PA, Aguiar MR. 2006 Extending point pattern analysis for objects of finite size and irregular shape. *J. Ecol.* **94**, 825–837. (doi:10.1111/j.1365-2745.2006.01113.x)

84. Wiegand T, Moloney KA, Naves J, Knauer F. 1999 Finding the missing link between landscape structure and population dynamics: a spatially explicit perspective. *Am. Nat.* **154**, 605–627. (doi:10.1086/303272)

85. Loosmore NB, Ford ED. 2006 Statistical inference using the G or K point pattern spatial statistics. *Ecology* **87**, 1925–1931. (doi:10.1890/0012-9658(2006)87[1925:SIUTGO]2.0.CO;2)

86. Levin SA. 1992 The problem of pattern and scale in ecology: the Robert H. MacArthur Award Lecture. *Ecology* **73**, 1943–1967. (doi:10.2307/1941447)

87. Besag J. 1974 Spatial interaction and the statistical analysis of lattice systems. *J. R. Stat. Soc. Ser. B* **36**, 192–225. (doi:10.1111/j.2517-6161.1974.tb00999.x)

88. Fraley C, Raftery AE. 2017 MCLUST Version 3 for R: Normal Mixture Modeling and Model-Based Clustering. (Vol. 504). Technical report.

89. Grabarnik P, Myllymäki M, Stoyan D. 2011 Correct testing of mark independence for marked point patterns. *Ecol. Modell.* **222**, 3888–3894. (doi:10.1016/j.ecolmodel.2011.10.005)

90. Fraley C, Raftery AE. 2007 Bayesian regularization for normal mixture estimation and model-based clustering. *J. Classif.* **24**, 155–181. (doi:10.1007/s00357-007-0004-5)

91. Pélissier R, Goreaud F. 2001 A practical approach to the study of spatial structure in simple cases of heterogeneous vegetation. *J. Veg. Sci.* **12**, 99–108. (doi:10.1111/j.1654-1103.2001.tb02621.x)

92. Chiu SN, Stoyan D, Kendall JM. 2013 Stochastic Geometry and Its Applications. Chichester, UK: Wiley.

93. Soznov NG, Bobkov NI, Mitchell EG, Kolesnikov AV, Grazhdankin DV. 2019 The ecology of *Dickinsonia* on tidal flats. *Estudi. Geol.* **75**, e116. (doi:10.3989/egeol.43587.571)

94. Kenkel NC. 1988 Pattern of self-thinning in jack pine: testing the random mortality hypothesis. *Ecology* **69**, 1017–1024. (doi:10.2307/1941257)

95. Ivantsov AY. 2013 Trace fossils of Precambrian metazoans 'Vendobionta' and 'Mollusks'. *Stratigr. Geol. Correl.* **21**, 252–264. (doi:10.1134/S0869593813030039)

96. Ivantsov AY. 2011 Feeding traces of Proarticulata—the Vendian Metazoa. *Paleontol. J.* **45**, 237–248. (doi:10.1134/S0031030111030063)

97. Ivantsov AY. 2009 New reconstruction of *Kimberella*, problematic Vendian metazoan. *Paleontol. J.* **43**, 601. (doi:10.1134/S003103010906001X)

98. Ivantsov AY, Malakhovskaya Y. 2002 Giant traces of Vendian animals. *Dokl. Earth Sci.* **385**, 618–622.

99. Managano MG, Buatois LA. 2017 The Cambrian revolutions: trace-fossil record, timing, links and geobiological impact. *Earth Sci. Rev.* **173**, 96–108. (doi:10.1016/j.earscirev.2017.08.009)

100. Hua H, Pratt BR, Zhang L-Y. 2003 Borings in *Cloudina* shells: complex predator-prey dynamics in the terminal Neoproterozoic. *Palaios* **18**, 454–459. (doi:10.1669/0883-1351(2003)018<0454:BICSCP>2.0.CO;2)

101. Giangrande A, Geraci S, Belmonte G. 1995 Life-cycle and life-history diversity in marine invertebrates and the implications in community dynamics. *Oceanographic Lit. Rev.* **8**, 662.

102. Liu AG, McIlroy D, Antcliffe JB, Brasier MD. 2011 Effaced preservation in the Ediacara biota and its implications for the early macrofossil record. *Palaeontology* **54**, 607–630. (doi:10.1111/j.1475-4983.2010.01024.x)

103. Darroch SAF, Laflamme M, Clapham ME. 2013 Population structure of the oldest known macroscopic communities from Mistaken Point, Newfoundland. *Paleobiology* **39**, 591–608. (doi:10.1666/12051)

104. Grazhdankin DV. 2003 Structure and depositional environment of the Vendian Complex in the southeastern White Sea area. *Stratigr. Geol. Correl.* **11**, 313–331.

105. Muscente AD *et al.* 2019 Ediacaran biozones identified with network analysis provide evidence for pulsed extinctions of early complex life. *Nat. Commun.* **10**, 1–15. (doi:10.1038/s41467-019-08837-3)

106. Grazhdankin DV, Balthasar U, Nagovitsin KE, Kochnev BB. 2008 Carbonate-hosted Avalon-type fossils in arctic Siberia. *Geology* **36**, 803–806. (doi:10.1130/G24946A.1)

107. Ben-Hur E, Kadmon R. 2020 Heterogeneity–diversity relationships in sessile organisms: a unified framework. *Ecol. Lett.* **23**, 193–207. (doi:10.1111/ele.13418)

108. Levin LA, Sibuet M, Gooday AJ, Smith CR, Vanreusel A. 2010 The roles of habitat heterogeneity in generating and maintaining biodiversity on continental margins: an introduction. *Mar. Ecol.* **31**, 1–5. (doi:10.1111/j.1439-0485.2009.00358.x)

109. Vanreusel A *et al.* 2010 The contribution of deep-sea macrohabitat heterogeneity to global nematode diversity. *Mar. Ecol.* **31**, 6–20. (doi:10.1111/j.1439-0485.2009.00352.x)

110. McClain C, Barry JP. 2010 Habitat heterogeneity, disturbance, and productivity work in concert to regulate biodiversity in deep submarine canyons. *Ecology* **91**, 964–976. (doi:10.1890/09-0087.1)

111. Sommer U. 2000 Benthic microalgal diversity enhanced by spatial heterogeneity of grazing. *Oecologia* **122**, 284–287. (doi:10.1007/PL00008857)

112. Stramski D, Rassoulzadegan F, Kiefer DA. 1992 Changes in the optical properties of a particle suspension caused by protist grazing. *J. Plankton Res.* **14**, 961–977. (doi:10.1093/plankt/14.7.961)

113. Leduc D, Rowden AA, Probert PK, Pilditch CA, Nodder SD, Vanreusel A, Duineveld GC, Witbaard R. 2012 Further evidence for the effect of particle-size diversity on deep-sea benthic biodiversity. *Deep Sea Res. Part I Oceanogr. Res. Pap.*. **63**, 164–169. (doi:10.1016/j.dsr.2011.10.009)

114. Gili J-M, Coma R. 1998 Benthic suspension feeders: their paramount role in littoral marine food webs. *Trends Ecol. Evol.* **13**, 316–321. (doi:10.1016/S0169-5347(98)01365-2)

115. Smith CR, De Leo FC, Bernardino AF, Sweetman AK, Arbizu PM. 2008 Abyssal food limitation, ecosystem structure and climate change. *Trends Ecol. Evol.* **23**, 518–528. (doi:10.1016/j.tree.2008.05.002)

116. Manno C, Stowasser G, Enderlein P, Fielding S, Tarling GA. 2015 The contribution of zooplankton faecal pellets to deep carbon transport in the Scotia Sea (Southern Ocean). *Biogeosciences* **12**, 1955–1965. (doi:10.5194/bg-12-1955-2015)

117. Davison PC, Checkley DM, Koslow JA, Barlow J. 2013 Carbon export mediated by mesopelagic fishes in the northeast Pacific Ocean. *Prog. Oceanogr.* **116**, 14–30. (doi:10.1016/j.pocean.2013.05.013)

118. Giering SLC *et al.* 2014 Reconciliation of the carbon budget in the ocean's twilight zone. *Nature* **507**, 480–483. (doi:10.1038/nature13123)

119. Monteiro PMS, Nelson G, van der Plas A, Mabille E, Bailey GW, Klingelhoeffer E. 2005 Internal tide—shelf topography interactions as a forcing factor governing the large-scale distribution and burial fluxes of particulate organic matter (POM) in the Benguela upwelling system. *Cont. Shelf Res.* **25**, 1864–1876. (doi:10.1016/j.csr.2005.06.012)